Potential stratospheric ozone depletion due to iodine injection from small satellites

Wuhu Feng, John M C Plane, Martyn P. Chipperfield, Alfonso Saiz-Lopez, Jean-paul Booth

Geophysical Research Letters

RESEARCH LETTER
10.1029/2022GL102300

Potential Stratospheric Ozone Depletion Due To Iodine Injection From Small Satellites

Wuhu Feng[1,2,3], John M. C. Plane[2], Martyn P. Chipperfield[3,4], Alfonso Saiz-Lopez[5], and Jean-Paul Booth[6]

[1]National Centre for Atmospheric Science (NCAS), University of Leeds, Leeds, UK, [2]School of Chemistry, University of Leeds, Leeds, UK, [3]School of Earth and Environment, University of Leeds, Leeds, UK, [4]National Centre for Earth Observation (NCEO), University of Leeds, Leeds, UK, [5]Department of Atmospheric Chemistry and Climate, Institute of Physical Chemistry Rocasolano, CSIC, Madrid, Spain, [6]Laboratoire de Physique des Plasma (LPP), CNRS, Sorbonne Universite, École Polytechnique, Institut Polytechnique de Paris, Palaiseau, France

Abstract We use the 3-D Whole Atmospheric Community Climate Model to investigate stratospheric ozone depletion due to the launch of small satellites (e.g., CubeSats) with an iodine propulsion system. The model considers the injection of iodine from the satellites into the Earth's thermosphere and suggests a 4-yr timescale for transport of the emissions down to the troposphere. The base case scenario is 40,000 small satellite launches per year into low orbit (100–600 km), which would inject 8 tons I yr^{-1} above 120 km as I^+ ions and increase stratospheric inorganic iodine by ~0.1 part per trillion (pptv). The model shows that this scenario produces a negligible impact on global stratospheric ozone (~0.05 DU column depletion). In contrast, a 100-fold increase in the launch rate, and therefore thermospheric iodine injection, is predicted to result in modeled ozone depletion of up to 14 DU (approximately 2%–7%) over the polar regions.

Plain Language Summary Iodine has the potential to cause stratospheric ozone depletion. Small satellites (<10 kg) in low Earth orbit require electric propulsion to prolong their time in orbit, and there is strong interest in replacing the rare gas propellant (Xe or Kr) with I_2. Here we estimate the potential impact of thermosphere iodine injection from such satellites on stratospheric ozone. Since the demand for small satellites could increase greatly in the future, it is important to understand the potential risks to ozone depletion if iodine propulsion systems are used. Assuming a scenario in which 40,000 small satellites are launched each year into relatively low orbits and each satellite is assumed to contain 200 g I_2, this could inject 8 tons/year of iodine ions into the upper atmosphere (above 120 km). Using a 3-D atmospheric chemistry-climate model, we show that the perturbation to the total column ozone is very small, decreasing by 0.05 DU (<0.02%) globally and 0.2 DU (<0.1%) for September/October in the Antarctic polar region. However, a 100-fold increase in the number of launches and therefore mass of iodine emitted into near-Earth orbit is predicted to cause significant ozone depletion up to 14 DU (5.6%) in the Antarctic spring.

Key Points:

- The effect of injecting iodine into the atmosphere from I_2-propelled satellites has been modeled using an atmosphere chemistry-climate model
- Injection of 8 tons I yr^{-1}, based on the expected launch rate, is predicted to cause negligible O_3 depletion (0.05 DU) globally
- O_3 depletion increases near-linearly with iodine mass injected, reaching up to 14 DU in the polar regions for 800 tons I yr^{-1}

Supporting Information:

Supporting Information may be found in the online version of this article.

Correspondence to:

W. Feng,
w.feng@ncas.ac.uk

Citation:

Feng, W., Plane, J. M. C., Chipperfield, M. P., Saiz-Lopez, A., & Booth, J.-P. (2023). Potential stratospheric ozone depletion due to iodine injection from small satellites. *Geophysical Research Letters*, *50*, e2022GL102300. https://doi.org/10.1029/2022GL102300

Received 29 NOV 2022
Accepted 5 FEB 2023

1. Introduction

The environmental impact of emissions from space launches has received much attention (Dallas et al., 2020) due to the space industry being one of the fastest growing global economic sectors (Ryan et al., 2022). Since the first assessment of the impact of rocket emissions by Cicerone and Stealman (1974), there have been many studies of the impacts of the Space Shuttle and similar rocket launches. They can inject significant quantities of gases and particles into the atmosphere (including chlorine compounds, H_2O, CO_2 and black carbon), potentially affecting ozone depletion, the dynamics of the atmosphere, and climate change (e.g., Larson et al., 2017; Maloney et al., 2022; Prather et al., 1990; Ross et al., 2009, 2010). The recent rapid growth in the number of satellite launches has been driven by the development of smaller satellites, particularly nanosatellites such as CubeSats which weigh less than 10 kg and are composed of one or more cube units (U) of 10 cm dimension (Twiggs, 2008; Villela et al., 2019). Almost 3900 CubeSats and nanosatellites were actively orbiting the Earth in 2022 (https://www.nanosats.eu/), comparable to the number of current operational satellites at low Earth orbit (4078) (https://ucsusa.org), but this is expected to rise significantly due to their lower launch costs (few tens of thousands to a million dollars, Villela et al., 2019). Rafalskyi et al. (2021) have recently developed an iodine electric propulsion system for small satellites, which has proved to perform better and cost less than using the more traditional xenon (or krypton) as a propellant (Bellomo et al., 2022). The first 12U CubeSat using this iodine electric propulsion

was launched in November 2021 into an orbit at ~480 km. The system produces iodine ions (I^+, I^{2+}, and I_2^+) after vaporizing solid iodine (Rafalskyi et al., 2021). Thus the launch of nanosatellites using iodine propulsion will inject gas-phase iodine species into the thermosphere, which upon re-entering the atmosphere could potentially cause depletion of the ozone layer and consequently impact climate. There is a need to evaluate this and other effects of space activities on the global atmosphere (e.g., Shutler et al., 2022).

Zafiriou (1974) first proposed that iodine, along with other active halogen atoms (Cl and Br), might react with ozone in the marine atmosphere. Chameides and Davis (1980) investigated the impact of iodine on the tropospheric photochemical system and the atmospheric ozone budget. Subsequently, Solomon et al. (1994) pointed out that iodine depletes ozone more efficiently than chlorine, and thus could be responsible for a significant contribution to past and future ozone changes. However, there are still uncertainties in the main gas- and condensed-phase iodine photochemical processes (see a comprehensive review in Saiz-Lopez et al. (2012)). So far, only a few global 3-D atmospheric models have included iodine chemistry (e.g., chemistry-climate models such as CAM by Ordóñez et al. (2012); SOCOL-AERv2-I by Karagodin-Doyennel et al. (2021); Whole Atmospheric Community Climate Model (WACCM) by Cuevas et al. (2022); and chemical transport models MOZART by Youn et al. (2010); TOMCAT/SLIMCAT by Hossaini et al. (2015); GEOS-Chem by Sherwen et al. (2016)). These models included the major sources of iodine from the Earth's surface (e.g., Carpenter, 2003; Carpenter et al., 2013; Jones et al., 2010; Saiz-Lopez et al., 2012). Recent measurements have indicated that up to 0.77 ± 0.10 parts per trillion by volume (pptv) total inorganic iodine is entrained into the stratosphere from the oceans (Koenig et al., 2020). These studies have shown that iodine may play an important role in stratospheric ozone depletion. However, there is still significant uncertainty concerning the magnitude of its effect, ranging from a few percent (e.g., Hossaini et al., 2015; Karagodin-Doyennel et al., 2021; Saiz-Lopez et al., 2015) to 10% (Cuevas et al., 2022). Indeed, the relative contribution of iodine could become more important (Cuevas et al., 2022; Klobas et al., 2021) due to the decreasing amounts of stratospheric chlorine and bromine as a result of the Montreal Protocol regulations (Feng et al., 2021).

In this paper, we implement and use a detailed atmospheric chemistry-climate model to assess and quantify the impact on ozone from the potential injection of iodine from nanosatellites equipped with iodine propulsion systems.

2. WACCM-Iodine

We have performed a series of experiments with WACCM (e.g., Marsh et al., 2013), which extends from the Earth's surface to about 140 km. The model contains a detailed description of chemistry in the troposphere, stratosphere, mesosphere and lower thermosphere (Emmons et al., 2020), including heterogeneous reactions on sulfate aerosols and polar stratospheric clouds (Solomon et al., 2015) as well as the very short-lived (VSL) halogen implementation (Cuevas et al., 2022). The halogen and VSL loading values used for 2014 are from WMO (2018). Here we use the same specified-dynamics (SD) version of WACCM (SD-WACCM), nudged with NASA's Modern Era Retrospective Analysis for Research and Application MERRA2 reanalysis data set (Molod et al., 2015) as in Cuevas et al. (2022). We follow the same default nudging scheme (Davis et al., 2020) in which only 1% of MERRA2 meteorological winds and temperature are combined with WACCM fields below 60 km at every model dynamic time step of 30 min (Feng et al., 2013). It is free-running above 60 km where the modeled temperature is calculated from the previous time step temperature and its tendencies from different processes (Smith et al., 2017).

In order to study the effect of the injection of iodine into the lower thermosphere by satellite propulsion systems, we have introduced four ion-molecule reactions involving I^+ and IO^+, with rate coefficients set to their modified Langevin capture rates using the statistical adiabatic channel model of Troe (1985). These reactions, together with a few additional neutral reactions that update the Cuevas et al. (2022) model, are listed in Table ST1 of the Supporting Information S1. The updated model therefore contains the iodine species I, I_2, IO, OIO, INO, INO_2, $IONO_2$, HI, HOI, I_2O_2, I_2O_3, I_2O_4, IBr, ICl, CH_3I, CH_2I_2, CH_2ICl, I^+, and IO^+. Total inorganic iodine (I_y) is defined as $I^+ + IO^+ + I + 2I_2 + IO + OIO + HI + HOI + INO + INO_2 + IONO_2 + IBr + ICl + 2I_2O_2 + 2I_2O_3 + 2I_2O_4$. The ionic iodine species were not considered in Karagodin-Doyennel et al. (2021) and Cuevas et al. (2022). For the base case scenario, we consider a steady-state nanosatellite population of 1,00,000, with a 2.5-year lifetime in orbit. This would require a launch rate of 40,000 per year. The propulsion system of each satellite is assumed to contain 200 g I_2, which corresponds to an injection of 8 tons of I^+ ions per year into the thermosphere. In our model, the I^+ is injected between 120 and 140 km, corresponding to a volumetric injection rate of 1.2×10^{-4} ions cm^{-3} s^{-1}. We assume there is no latitudinal or seasonal variation of the I^+ injection.

Table 1
WACCM Model Experiments

Experiments	Description	Thermosphere iodine injection (TII) rate from small satellites	Iodine surface emissions
CNTL (or TII0)	Control experiment	None	Surface emissions are the same as Cuevas et al. (2022), while the surface emission of CF_3I is from Zhang et al. (2020)
TII1	As CNTL, but considering the base scenario of TII from small satellites (see main text)	1.2×10^{-4} cm^{-3} s^{-1} above 120 km	Same as CNTL
TII10	As TII1, but assuming 10 times of TII1 from small satellites	1.2×10^{-3} cm^{-3} s^{-1} above 120 km	Same as CNTL
TII100	As TII1, but assuming 100 times of TII1 from small satellites	1.2×10^{-2} cm^{-3} s^{-1} above 120 km	Same as CNTL
TII1_S0	As TII1 but without any surface iodine emissions	1.2×10^{-4} cm^{-3} s^{-1} above 120 km	None
TII10_S0	As TII10 but without any surface iodine emissions	1.2×10^{-3} cm^{-3} s^{-1} above 120 km	None
TII100_S0	As TII100 but without any surface iodine emissions	1.2×10^{-2} cm^{-3} s^{-1} above 120 km	None

We performed a total of seven time-slice model simulations (see Table 1). The control run (CNTL) included the iodine chemistry described above but without any injection of I^+ from the thermosphere (zero Thermosphere Iodine Injection, TII0). The six sensitivity runs use the same model as CNTL but include thermospheric injection of I^+ for the base case scenario (TII1), which was then increased by factors of 10 (TII10) and 100 (TII100). Increasing up to 100 times is done to establish the trend, so that the impact of any future increase can be assessed. These runs also included surface emissions of both inorganic (HOI, I_2) and organic (CH_3I, CH_2I_2, CH_2IBr, and CH_2ICl) species as in Cuevas et al. (2022). The surface emission of CF_3I is from Zhang et al. (2020). A further three model simulations were similar but without the surface iodine emission (S0); these are labeled TII1_S0, TII10_S0, and TII100_S0. All of these simulations are perpetual runs representative of year 2014, so that all conditions (such as surface emissions, meteorological reanalysis fields and solar input) were identical, to greatly reduce inter-annual variations. The current work has not investigated the column ozone abundance changes from the inter-annual dynamical variability (e.g., Chipperfield et al., 2018; Weber et al., 2011). Each simulation is a 15-year time-slice run, and only the final 5 years of simulation are used for the analysis. The runs CNTL, TII1, TII10, and TII100 use the same initialization from Cuevas et al. (2022), while the runs TII1_S0, TII10_S0, and TII100_S0 use the initialization files without any iodine species from the standard WACCM4 simulation for 2014. All WACCM simulations used 88 vertical levels at 1.9° × 2.5° horizontal resolution. The monthly mean model output was saved for analysis.

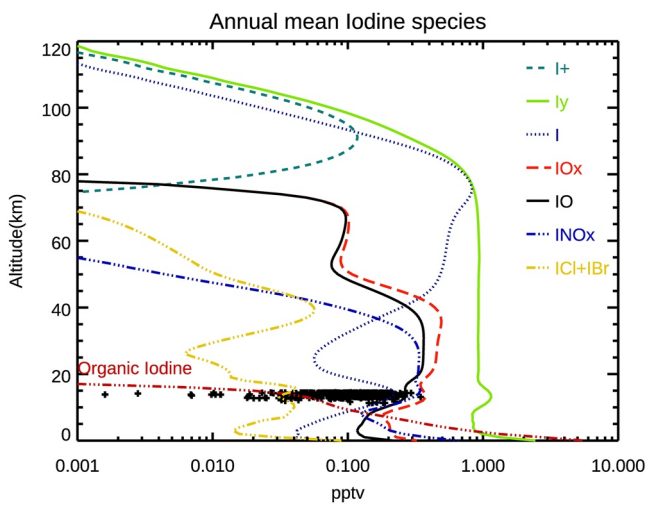

Figure 1. Global mean annual mean profiles of the major iodine-containing species (see legend) from WACCM run CNTL (see Table 1) using the final 5 years of the perpetual 2014 simulation. Also shown is the observed IO (140°–152°E, 20°S–40°N, 24 January–25 February 2014) from the Airborne Multi-Axis Differential Optical Absorption Spectroscopy (AMAX-DOAS, + symbols) (Koenig et al., 2020).

3. Results

We compare our CNTL model simulation results to measurements of iodine oxide (IO) obtained by the Airborne Multi-Axis Differential Optical Absorption Spectroscopy instrument (Koenig et al., 2020). The merged satellite measurements of the total column ozone (TOZ) and ozone profiles were obtained from the Copernicus Climate Change Service (C3S) product at https://cds.climate.copernicus.eu/cdsapp#!/dataset/satellite-ozone?tab=form.

3.1. Iodine Partitioning

Figure 1 shows the global mean annual mean vertical profiles of the major iodine species from the model control simulation (CNTL). As expected, with the inclusion of the updated iodine chemistry (Table ST1 in Supporting Information S1), I^+ is the dominant species above 90 km. IO^+ occurs in a layer that peaks (at less than 10^{-4} pptv, not shown) around 80 km. Neutral atomic iodine I is dominant in the upper stratosphere to the lower thermosphere. IO_x

(=IO + OIO + $2I_2O_2$ + $2I_2O_3$ + $2I_2O_4$) and INO_x (=INO + INO_2 + $IONO_2$) dominate the total inorganic iodine in the stratosphere, where there are small (negligible) amounts of other I_y species (ICl, IBr) and organic iodine (=CH_3I + CF_3I + $2CH_2I_2$ + CH_2IBr + CH_2ICl). The presence of IO in the atmosphere is important for the lower stratospheric ozone depletion (e.g., Solomon et al., 1994), and the simulation CNTL reproduces the observed IO (Koenig et al., 2020) quite well (see also Figure S1 in Supporting Information S1).

3.2. Residence Time

It is important to estimate the timescale for transport of iodine injected into the lower thermosphere to reach the troposphere and be removed by washout and dry deposition. The atmospheric residence time can be defined as the ratio of the total mass of atmospheric iodine (in a simulation which considers nanosatellites iodine injection as the only source) divided by the input flux above 120 km. Figure S2 in Supporting Information S1 shows the annual mean I_y total column abundance for the 15th year of simulation from runs TII1_S0 simulation (top panel) and the ratio between the corresponding simulations of TII10_S0 (middle), TII100_S0 (bottom), and TII1_S0. A large I_y column density occurs in the polar regions (8–11.2 × 10^{10} cm^{-2} and 5–7.6 × 10^{10} cm^{-2} in the southern (SH) and northern hemispheres (NH), respectively), whereas the I_y column in the tropics is smaller (~1.5 × 10^{10} cm^{-2}), (recall that these simulations do not include surface sources of iodine). Obviously, the I_y column density from TII1_S0 is much smaller than from the CNTL simulation. As expected, the modeled I_y abundance is nearly proportional to the thermospheric I^+ injection rate, indicating that the residence time of iodine is very similar for these different injection rates, being about 4 years once the simulations have spun-up (Figure S3 in Supporting Information S1). There is evidence of a small feedback effect, with slightly shorter residence times for the larger injection rates.

3.3. Impact of Nanosatellites on Iodine Abundance

Figure 2 shows the latitude-height (10–120 km) annual mean zonal mean I_y from the control simulation CNTL and the differences induced by different injection rate scenarios. The global mean modeled I_y in simulation CNTL

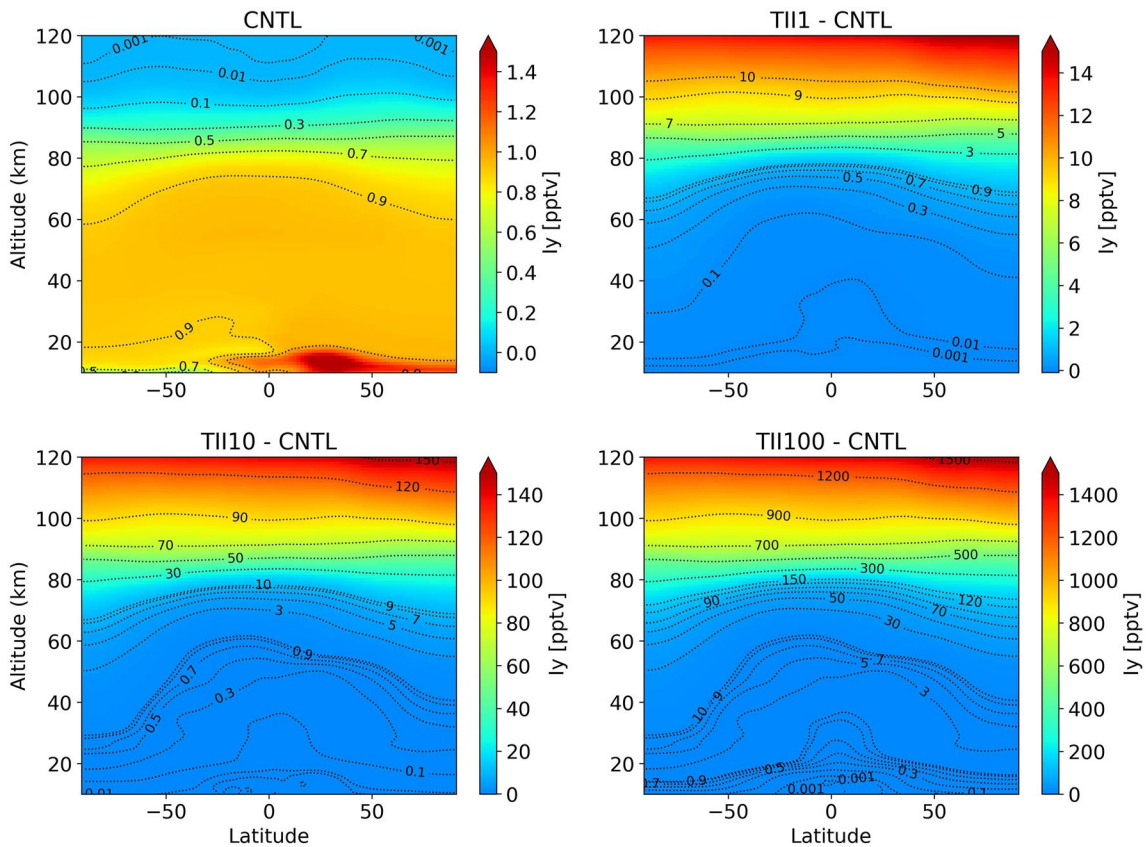

Figure 2. Annual mean zonal mean I_y (pptv) from the WACCM control (CNTL) simulation and the absolute differences between CNTL and simulations TII1, TII10, and TII100. These simulations consider iodine sources both in the thermosphere from small satellites with an iodine propulsion system and surface emissions (see Table 1).

has little latitudinal variation throughout the stratosphere to lower mesosphere, and the value of 0.9 pptv is close to the upper limit value of 0.87 pptv (0.77 ± 0.10) derived from aircraft measurements (Koenig et al., 2020) (little latitudinal varations above upper stratosphere are also seen in the model simulations without surface sources of iodine (Figure S4 in Supporting Information S1)). When thermospheric injection is added, the modeled I_y mixing ratio increases with altitude to the lower thermosphere where the injection occurs in the model, and shows an almost linear proportionality to the rate of I^+ injection. This additional I_y occurs mainly in the form of neutral species below 80 km (Figure S5 in Supporting Information S1) and in the form of ionized iodine species above ~80 km (Figure 1), respectively. Stratospheric iodine also increases; for example, there is an additional 0.1, 1, and 10 pptv of I_y at 30 km at high southern latitudes for the three injection scenarios of TII1, TII10, and TII100, respectively. Interestingly, there are two layers of I from the CNTL simulation, one in the tropical stratosphere with 0.3–0.4 pptv and the other in the lower mesosphere around 75 km with 0.8 pptv. The latter has not been reported before to our knowledge. Figures S6 and S7 in Supporting Information S1 are the similar plots for IO_x and INO_x, which represent the dominant species involved with stratospheric ozone depletion. Clearly, as the rate of injection of iodine increases, more IO_x and INO_x are produced in the stratosphere, with the potential to destroy more ozone.

3.4. Impact of Nanosatellites on Ozone

Figure 3 shows the observed TOZ from the merged satellite data set C3S and SBUV instrument (https://acd-ext.gsfc.nasa.gov/Data_services/merged/), averaged for three latitude regions, compared to the WACCM control simulation CNTL. Also shown are the corresponding absolute TOZ differences under different scenarios. The seasonal evolution of TOZ is well captured by simulation CNTL, though there are some differences in the absolute amount. Cuevas et al. (2022) argued that including iodine chemistry in WACCM improved the simulation of observed TOZ (also see Figures S8–S10 in Supporting Information S1). There is only a very small decrease in TOZ with the iodine injection rate of the base case scenario (TII1) which assumes an injection of 8 tons per year of I^+ ions into the thermosphere.

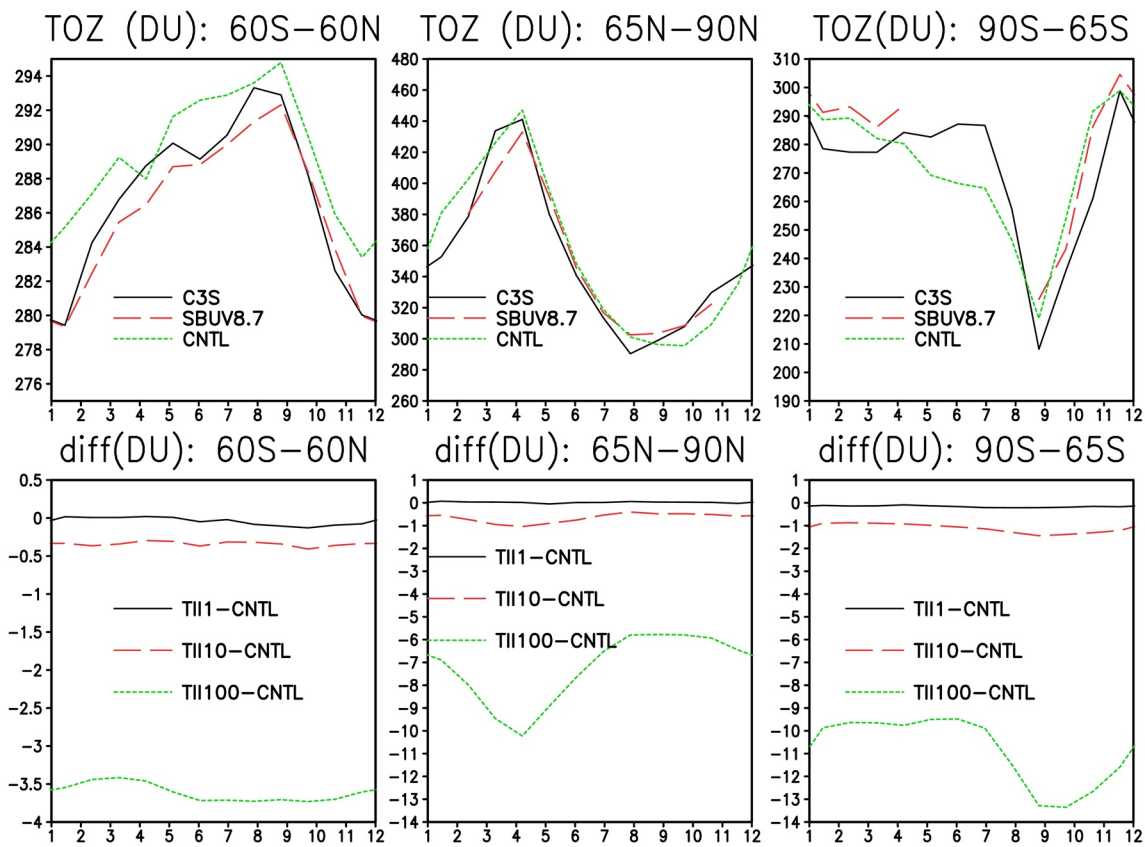

Figure 3. Top panels: seasonal variation of mean column ozone (DU) averaged over (left) near global mean, (middle) northern hemisphere high latitudes and (right) southern hemisphere high latitudes from measurements and the model control simulation (CNTL). Lower panels: The corresponding absolute difference in total column ozone (DU) between the model simulations under different rates of injection of thermosphere iodine from small satellites (see Table 1) and CNTL.

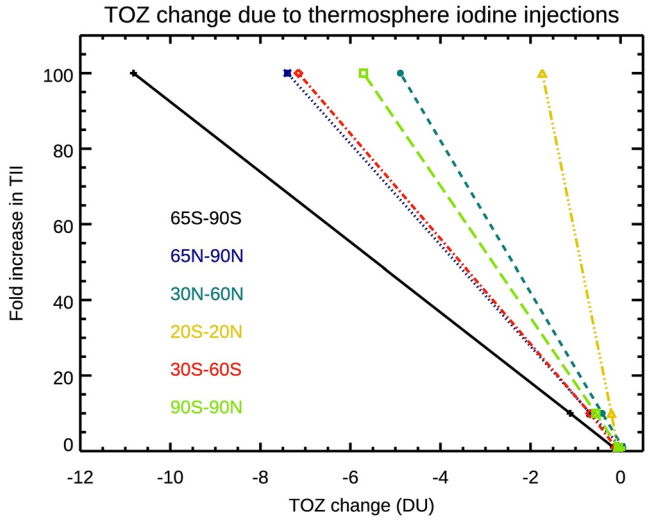

Figure 4. Annual mean total column ozone change (DU) with respect to the model control simulation (CNTL) for different thermosphere iodine injection (TII) scenarios from small satellites over different latitude regions (see legend and Table ST2 in Supporting Information S1).

As expected, larger ozone decreases are predicted with larger injected quantities of iodine; around 1 DU (0.2%–0.7%) for TII10, and 10–14 DU (3%–7.5%) and 6–10 DU (~2%) from TII100 in the SH and NH high latitudes, respectively (also see Figures S11 and S12 in Supporting Information S1).

Figure 4 summarizes the modeled annual mean TOZ changes for different scenarios over different latitude regions. The increase in ozone depletion with increasing iodine injection is clearly seen. There are small oscillations in the TOZ changes withTII, which likely reflect the small impact compared to dynamic variability of the model (see also Tables ST2 and ST3 in Supporting Information S1). The increased ozone depletion that would be caused by an increasing number of small satellites in low Earth orbit with iodine propulsion systems is clearly modeled in all latitude regions. The smallest depletion occurs in the tropical region, and largest occurs in the polar regions, especially in the lower stratosphere in the Antarctic (see Figures S10 and S11 in Supporting Information S1), which is mainly caused by the coupling between iodine and other reaction cycles including chlorine, bromine, O_x, NO_x, and HO_x. Larger amounts of IO_x and INO_x are produced at high latitudes (see Figures S6 and S7 in Supporting Information S1), which dominate the total I_y in the lower stratosphere (Figure 1).

4. Discussion and Conclusions

Following the first launch into a low orbit of a CubeSat which uses an iodine electric propulsion in November 2021, it is important to understand the potential risks to stratospheric ozone. To accomplish this, we have added a treatment of iodine injection and additional neutral as well as ion chemistry to WACCM-Iodine model. We have performed a number of perpetual model runs with different additional scenarios of iodine injection at 120–140 km to explore the potential stratospheric ozone depletion from small satellites powered in this way. For the base case scenario, a steady-state nanosatellite launch rate of 40,000/year (e.g., assuming 8 tons of I^+ injected), the perturbation to the TOZ is negligible. However, a 100-fold increase in the mass of iodine injected into near-Earth orbit will cause significant ozone depletion. This study quantifies the extent to which the injection of iodine into the thermosphere can deplete stratospheric ozone, which may assist regulatory authorities in assessing the ozone impact of iodine-propelled satellites in low Earth orbit.

Data Availability Statement

IO observations is available from https://doi.org/10.5065/D6F769MF. The merged satellite measurements of total column ozone and Microwave Limb Sounder (MLS) ozone profiles are obtained from https://cds.climate.copernicus.eu/cdsapp#!/dataset/satellite-ozone?tab=form. SBUV total column ozone is available at https://acd-ext.gsfc.nasa.gov/Data_services/merged. All data used in this paper, including the model results, are available from https://doi.org/10.5281/zenodo.7588817.

Acknowledgments
This work was supported by the NERC projects NE/V011863/1, NE/R011222/1 and also partly supported by Fédération de recherche PLAS@PAR. We thank Dr Carlos Cuevas for providing WACCM-Iodine model source code and related input data. We thank Drs Ryan Hossaini and Xin Zhou for helpful discussions. The model simulations were performed on the Leeds ARC HPC facilities.

References

Bellomo, N., Magarotto, M., Manente, M., Trezzolani, F., Mantellato, R., Cappellini, L., et al. (2022). Design and in-orbit demonstration of REGULUS, an iodine electric propulsion system. *CEAS Space Journal*, *14*(1), 79–90. https://doi.org/10.1007/s12567-021-00374-4

Carpenter, L. J. (2003). Iodine in the marine boundary layer. *Chemical Reviews*, *103*(12), 4953–4962. https://doi.org/10.1021/cr0206465

Carpenter, L. J., MacDonald, S. M., Shaw, M. D., Kumar, R., Saunders, R. W., Parthipan, R., et al. (2013). Atmospheric iodine levels influenced by sea surface emissions of inorganic iodine. *Nature Geoscience*, *6*(2), 108–111. https://doi.org/10.1038/ngeo1687

Chameides, W. L., & Davis, D. D. (1980). Iodine: Its possible role in tropospheric photochemistry. *Journal of Geophysical Research*, *85*(C12), 7383–7398. https://doi.org/10.1029/JC085iC12p07383

Chipperfield, M. P., Dhomse, S., Hossaini, R., Feng, W., Santee, M. L., Weber, M., et al. (2018). On the cause of recent variations in lower stratospheric ozone. *Geophysical Research Letters*, *45*(11), 5718–5726. https://doi.org/10.1029/2018GL0787071

Cicerone, R. J., & Stealman, D. H. (1974). The space shuttle and other atmospheric chlorine sources. *Paper presented at the 6th conference on aerospace and aeronautical meteorology* (pp. 12–15). American Meteorological Society.

Cuevas, C. A., Fernandez, R. P., Kinnison, D. E., Li, Q., Lamarque, J.-F., Trabelsi, T., et al. (2022). The influence of iodine on the Antarctic stratospheric ozone hole. *Proceedings of the National Academy of Sciences of the United States of America*, *119*(7). https://doi.org/10.1073/pnas.2110864119

Dallas, J. A., Raval, S., Alvarez Gaitan, J. P., Saydam, S., & Dempster, A. G. (2020). The environmental impact of emissions from space launches: A comprehensive review. *Journal of Cleaner Production*, *255*, 2020. https://doi.org/10.1016/j.jclepro.2020.120209

Davis, N. A., Davis, S. M., Portmann, R. W., Ray, E., Rosenlof, K. H., & Yu, P. (2020). A comprehensive assessment of tropical stratospheric upwelling in the specified dynamics Community Earth System Model 1.2.2—Whole Atmosphere Community Climate Model (CESM (WACCM)). *Geoscientific Model Development*, *13*(2), 717–734. https://doi.org/10.5194/gmd-13-717-2020

Emmons, L. K., Schwantes, R. H., Orlando, J. J., Tyndall, G., Kinnison, D., Lamarque, J.-F., et al. (2020). The chemistry mechanism in the community Earth system model version 2 (CESM2). *Journal of Advances in Modeling Earth Systems*, *12*(4), e2019MS001882. https://doi.org/10.1029/2019MS001882

Feng, W., Dhomse, S. S., Arosio, C., Weber, M., Burrows, J. P., Santee, M. L., & Chipperfield, M. P. (2021). Arctic ozone depletion in 2019/20: Roles of chemistry, dynamics and the Montreal Protocol. *Geophysical Research Letters*, *48*(4), e2020GL091911. https://doi.org/10.1029/2020GL091911

Feng, W., Marsh, D. R., Chipperfield, M. P., Janches, D., Höffner, J., Yi, F., & Plane, J. M. C. (2013). A global atmospheric model of meteoric iron. *Journal of Geophysical Research: Atmospheres*, *118*(16), 9456–9474. https://doi.org/10.1002/jgrd.50708

Hossaini, R., Chipperfield, M. P., Montzka, S., Rap, A., Dhomse, S., & Feng, W. (2015). Efficiency of short-lived halogens at influencing climate through depletion of stratospheric ozone. *Nature Geoscience*, *8*(3), 186–190. https://doi.org/10.1038/ngeo2363

Jones, C. E., Hornsby, K. E., Sommariva, R., Dunk, R. M., von Glasow, R., McFiggans, G., & Carpenter, L. J. (2010). Quantifying the contribution of marine organic gases to atmospheric iodine. *Geophysical Research Letters*, *37*(18), L18804. https://doi.org/10.1029/2010GL043990

Karagodin-Doyennel, A., Rozanov, E., Sukhodolov, T., Egorova, T., Saiz-Lopez, A., Cuevas, C. A., et al. (2021). Iodine chemistry in the chemistry–climate model SOCOL-AERv2-I. *Geoscientific Model Development*, *14*(10), 6623–6645. https://doi.org/10.5194/gmd-14-6623-2021

Klobas, J. K., Hansen, J., Weisenstein, D. K., Kennedy, R. P., & Wilmouth, D. M. (2021). Sensitivity of iodine-mediated stratospheric ozone loss chemistry to future chemistry-climate scenarios. *Frontiers of Earth Science*, *9*. https://doi.org/10.3389/feart.2021.617586

Koenig, T. K., Baidar, S., Campuzano-Jost, P., Cuevas, C. A., Dix, B., Fernandez, R. P., et al. (2020). Quantitative detection of iodine in the stratosphere. *Proceedings of the National Academy of Sciences of the United States of America*, *117*(4), 1860–1866. https://doi.org/10.1073/pnas.1916828117

Larson, E. J. L., Portmann, R. W., Rosenlof, K. H., Fahey, D. W., Daniel, J. S., & Ross, M. N. (2017). Global atmospheric response to emissions from a proposed reusable space launch system. *Earth's Future*, *5*(1), 37–48. https://doi.org/10.1002/2016EF000399

Maloney, C. M., Portmann, R. W., Ross, M. N., & Rosenlof, K. H. (2022). The climate and ozone impacts of black carbon emissions from global rocket launches. *Journal of Geophysical Research: Atmospheres*, *127*(12), e2021JD036373. https://doi.org/10.1029/2021JD036373

Marsh, D. R., Mills, M. J., Kinnison, D. E., Lamarque, J., Calvo, N., & Polvani, L. M. (2013). Climate change from 1850 to 2005 simulated in CESM1(WACCM). *Journal of Climate*, *26*(19), 7372–7391. https://doi.org/10.1175/jcli-d-12-00558.1

Molod, A., Takacs, L., Suarez, M., & Bacmeister, J. (2015). Development of the GEOS-5 atmospheric general circulation model: Evolution from MERRA to MERRA2. *Geoscientific Model Development*, *8*(5), 1339–1356. https://doi.org/10.5194/gmd-8-1339-2015

Ordóñez, C., Lamarque, J.-F., Tilmes, S., Kinnison, D. E., Atlas, E. L., Blake, D. R., et al. (2012). Bromine and iodine chemistry in a global chemistry-climate model: Description and evaluation of very short-lived oceanic sources. *Atmospheric Chemistry and Physics*, *12*(3), 1423–1447. https://doi.org/10.5194/acp-12-1423-2012

Prather, M. J., García, M. M., Douglass, A. R., Jackman, C. H., Ko, M. K. W., & Sze, N. D. (1990). The space shuttle's impact on the stratosphere. *Journal of Geophysical Research*, *95*(D11), 18583–18590. https://doi.org/10.1029/JD095iD11p18583

Rafalskyi, D., Martínez, J. M., Habl, L., Zorzoli Rossi, E., Proynov, P., Bore, A., et al. (2021). In-orbit demonstration of an iodine electric propulsion system. *Nature*, *599*(7885), 411–415. https://doi.org/10.1038/s41586-021-04015-y

Ross, M., Mills, M., & Toohey, D. (2010). Potential climate impact of black carbon emitted by rockets. *Geophysical Research Letters*, *37*(24), L24810. https://doi.org/10.1029/2010GL044548

Ross, M., Toohey, D., Peinemann, M., & Ross, P. (2009). Limits on the space launch market related to stratospheric ozone depletion. *Astropolitics*, *7*(1), 50–82. https://doi.org/10.1080/14777620902768867

Ryan, R. G., Marais, E. A., Balhatchet, C. J., & Eastham, S. D. (2022). Impact of rocket launch and space debris air pollutant emissions on stratospheric ozone and global climate. *Earth's Future*, *10*(6), e2021EF002612. https://doi.org/10.1029/2021EF002612

Saiz-Lopez, A., Baidar, S., Cuevas, C. A., Koenig, T. K., Fernandez, R. P., Dix, B., et al. (2015). Injection of iodine to the stratosphere. *Geophysical Research Letters*, *42*(16), 6852–6859. https://doi.org/10.1002/2015GL064796

Saiz-Lopez, A., Plane, J. M. C., Baker, A. R., Carpenter, L. J., von Glasow, R., Gómez Martín, J. C., et al. (2012). Atmospheric chemistry of iodine. *Chemical Reviews*, *112*(3), 1773–1804. https://doi.org/10.1021/cr200029u

Sherwen, T., Evans, M. J., Carpenter, L. J., Andrews, S. J., Lidster, R. T., Dix, B., et al. (2016). Iodine's impact on tropospheric oxidants: A global model study in GEOS-chem. *Atmospheric Chemistry and Physics*, *16*(2), 1161–1186. https://doi.org/10.5194/acp-16-1161-2016

Shutler, J. D., Yan, X., Cnossen, I., Schulz, L., Watson, A. J., GlaBmeier, K. H., et al. (2022). Atmospheric impacts of the space industry require oversight. *Nature Geoscience*, *15*(8), 598–600. https://doi.org/10.1038/s41561-022-01001-5

Smith, A. K., Pedatella, N. M., Marsh, D. R., & Matsuo, T. (2017). On the dynamical control of the mesosphere-lower thermosphere by the lower and middle atmosphere. *Journal of the Atmospheric Sciences*, *74*(3), 933–947. https://doi.org/10.1175/JAS-D-16-0226.1

Solomon, S., Garcia, R. R., & Ravishankara, A. R. (1994). On the role of iodine in ozone depletion. *Journal of Geophysical Research*, *99*(D10), 20491–20499. https://doi.org/10.1029/94JD02028

Solomon, S., Kinnison, D., Bandoro, J., & Garcia, R. (2015). Simulation of polar ozone depletion: An update. *Journal of Geophysical Research: Atmospheres*, *120*(15), 7958–7974. https://doi.org/10.1002/2015JD023365

Troe, J. (1985). Statistical adiabatic channel model of ion-neutral dipole capture rate constants. *Chemical Physics Letters*, *122*(5), 425–430. https://doi.org/10.1016/0009-2614(85)87240-7

Twiggs, R. (2008). Origin of CubeSat. In H. Helvajian, & S. W. Janson (Eds.), *Small satellite: Past, present, and future* (pp. 151–173). The Aerospace Press.

Villela, T., Costa, C. A., Brandão, A. M., Bueno, F. T., & Leonardi, R. (2019). Towards the thousandth CubeSat: A statistical overview. *International Journal of Aerospace Engineering*, *2019*, 5063145–5063213. https://doi.org/10.1155/2019/5063145

Weber, M., Dikty, S., Burrows, J. P., Garny, H., Dameris, M., Kubin, A., et al. (2011). The Brewer-Dobson circulation and total ozone from seasonal to decadal time scales. *Atmospheric Chemistry and Physics*, *11*(21), 11221–11235. https://doi.org/10.5194/acp-11-11221-2011

WMO. (2018). World Meteorological Organization (WMO)/United Nations Environment Programme (UNEP). In *Scientific assessment of ozone depletion: 2018 global ozone research and monitoring project report No 58* (p. 588). World Meteorological Organization.

Youn, D., Patten, K. O., Wuebbles, D. J., Lee, H., & So, C.-W. (2010). Potential impact of iodinated replacement compounds CF_3I and CH_3I on atmospheric ozone: A three-dimensional modeling study. *Atmospheric Chemistry and Physics*, *10*(20), 10129–10144. https://doi.org/10.5194/acp-10-10129-2010

Zafiriou, O. C. (1974). Photochemistry of halogens in the marine atmosphere. *Journal of Geophysical Research*, *79*(18), 2730–2732. https://doi.org/10.1029/JC079i018p02730

Zhang, J., Wuebbles, D. J., Kinnison, D. E., & Saiz-Lopez, A. (2020). Revising the ozone depletion potentials metric for short-lived chemicals such as CF_3I and CH_3I. *Journal of Geophysical Research: Atmospheres*, *125*(9), e2020JD032414. https://doi.org/10.1029/2020JD032414

References From the Supporting Information

Bones, D., Plane, J. M. C., & Feng, W. (2015). Dissociative recombination of FeO^+ with electrons: Implications for plasma layers in the ionosphere. *Journal of Physical Chemistry A*, *120*(9), 1369–1376. https://doi.org/10.1021/acs.jpca.5b04947

Lide, D. R. (2006). *Handbook of physics and chemistry*. CRC Press.